

One jet to rule them all: monojet constraints and invisible decays of a 750 GeV diphoton resonance.

Daniele Barducci,^a Andreas Goudelis,^b Suchita Kulkarni^b and Dipan Sengupta^c

^a*LAPTh, Université Savoie Mont Blanc, CNRS,
B.P. 110, F-74941 Annecy-le-Vieux, France*

^b*Institute of High Energy Physics, Austrian Academy of Sciences,
Nikolsdorfergasse 18, 1050 Vienna, Austria*

^c*Laboratoire de Physique Subatomique et de Cosmologie, Université Grenoble-Alpes,
CNRS/IN2P3, 53 Avenue des Martyrs, F-38026 Grenoble, France*

E-mail: daniele.barducci@lapth.cnrs.fr,
andreas.goudelis@oeaw.ac.at, suchita.kulkarni@oeaw.ac.at,
dipan.sengupta@lpsc.in2p3.fr

ABSTRACT: The ATLAS and CMS collaborations recently reported a mild excess in the diphoton final state pointing to a resonance with a mass of around 750 GeV and a potentially large width. We consider the possibility of a scalar resonance being produced via gluon fusion and decaying to electroweak gauge bosons, jets and pairs of invisible particles, stable at collider scales. We compute limits from monojet searches on such a resonance and test their compatibility with the requirement for a large width. We also study whether the stable particle can be a dark matter candidate and investigate the corresponding relic density constraints along with the collider limits. We show that monojet searches rule out a large part of the available parameter space and point out scenarios where a broad diphoton resonance can be reconciled with monojet constraints.

Contents

1	Introduction	1
2	Working assumptions, collider and DM constraints	2
2.1	Effective description of a 750 GeV resonance	2
2.2	Collider implications and observational status	3
2.3	Dark matter and a (pseudo-)scalar portal at 750 GeV	4
3	Analysis	5
3.1	Analysis setup	5
3.2	Results	7
4	Summary and conclusions	12
5	Acknowledgements	13
A	Some comments on potential UV completions	13
B	Some more details on direct detection	15

1 Introduction

The ATLAS [1] and CMS [2] collaborations recently announced their first results on searches for new resonances decaying into two photons at 13 TeV centre-of-mass (CM) energy pp collisions, with integrated luminosities of 3.2 fb^{-1} and 2.6 fb^{-1} respectively. They both observe an excess of events in the diphoton invariant mass bins around 750 GeV, with a 3.6σ (2.0σ) and 2.6σ (1.2σ) local (global) significance respectively. A large number of papers have already appeared, studying potential implications of such an observation and numerous ways to interpret it in terms of New Physics (NP) scenarios [3–49].

The situation is of course still extremely uncertain, partly because of the low significance of the excess which could be due to a statistical fluctuation. Still, it is interesting to examine various facets of the consequences of such an observation being confirmed in the near future. A first statement that can be made with some certainty is that if indeed a new particle is being observed in the diphoton channel, it should have spin-0 or 2 by virtue of the Landau-Yang theorem [50, 51] (see, however, [46, 47]). In this work we focus on the spin-0 case. On the slightly more speculative side, the excess appears to be compatible with fairly large cross section values, lying

at the limits of (although surviving) the LHC Run-1 constraints. Lastly, it looks compatible with a particle of a fairly large width, with first estimates even pointing to a particle as broad as 45 GeV [1].

It has already been shown (see, *e.g.*, [38]) that decays into Standard Model (SM) particles alone cannot account for a width as large as 45 GeV. One interesting way through which a broad resonance can be explained is by invoking decays into some invisible final state. If, moreover, these final state particles are also stable on cosmological timescales, then one could eventually entertain the possibility that they may constitute the dark matter (DM) in the Universe, while the resonance itself could actually play the role of a “portal” between the SM particles and the DM sector [52]. Needless to say, this portal scenario could in principle also be viable even if the resonance turns out to be narrow.

This simple picture is, nonetheless, subject to numerous constraints. First, the coupling of the resonance to gluons or quarks is constrained (albeit weakly) by LHC dijet searches at 8 TeV. Then, the decays into invisible states are subject to bounds from the monojet + missing energy ($j + E_T^{\text{miss}}$) searches, which are the main topic of this paper. Finally, if one wishes to make a connection to DM physics, then one should examine the compatibility of all the LHC constraints with those coming from DM abundance considerations and, eventually, direct/indirect detection.

In this paper we make an effort to put some of these pieces together in a systematic manner. We recast a supersymmetry (SUSY) monojet search to obtain constraints on the parameter space of the considered model and show their interplay with the diphoton resonance production cross section, its decay width into invisible final states, 13 TeV dijet cross section predictions as well as with cosmological considerations on DM. The paper is organised as follows: in Sec. 2 we describe our parametrisation for the resonance interactions with SM and invisible particles, summarise the experimental situation on the collider side and comment on DM-related properties. In Sec. 3 we describe the setup of our analysis, the tools we employ and present our main findings. Finally, in Sec. 4 we summarise our results and conclude.

2 Working assumptions, collider and DM constraints

2.1 Effective description of a 750 GeV resonance

Our working assumption is that the observed excess around 750 GeV is due to a SM gauge singlet scalar particle s that (effectively) couples to the SM gluons and electroweak (EW) gauge bosons, as well as to a new species of Majorana fermions ψ . We neglect all potential couplings of s to SM fermions (which, for a singlet s , can also only arise through higher-dimensional operators) as well as to the 125 GeV Higgs boson (which are allowed at tree-level).

Numerous conventions have been adopted by different authors in order to describe such effective interactions. We choose to parametrise our Lagrangian as¹

$$\begin{aligned} \mathcal{L}_{\text{NP,CPE}} = & \frac{1}{2}(\partial_\mu s)^2 - \frac{\mu_s^2}{2}s^2 + \frac{1}{2}\bar{\psi}(i\not{\partial} - m_\psi)\psi - \frac{y_\psi}{2}s\bar{\psi}\psi \\ & - \frac{g_1^2}{4\pi} \frac{1}{4\Lambda_1} s B_{\mu\nu} B^{\mu\nu} - \frac{g_2^2}{4\pi} \frac{1}{4\Lambda_2} s W_{\mu\nu} W^{\mu\nu} - \frac{g_3^2}{4\pi} \frac{1}{4\Lambda_3} s G_{\mu\nu} G^{\mu\nu} \end{aligned} \quad (2.1)$$

where $B_{\mu\nu}$, $W_{\mu\nu}$ and $G_{\mu\nu}$ are the $U(1)_Y$, $SU(2)_L$ and $SU(3)_c$ field strength tensors respectively and $g_{1,2,3}$ are the corresponding SM coupling constants. The Lagrangian (2.1) actually corresponds to the case where s is even under the charge-parity (CP) symmetry. In the case of a pseudoscalar particle, the Lagrangian becomes

$$\begin{aligned} \mathcal{L}_{\text{NP,CPO}} = & \frac{1}{2}(\partial_\mu s)^2 - \frac{\mu_s^2}{2}s^2 + \frac{1}{2}\bar{\psi}(i\not{\partial} - m_\psi)\psi - i\frac{y_\psi}{2}s\bar{\psi}\gamma^5\psi \\ & - \frac{g_1^2}{4\pi} \frac{1}{4\Lambda_1} s B_{\mu\nu} \tilde{B}^{\mu\nu} - \frac{g_2^2}{4\pi} \frac{1}{4\Lambda_2} s W_{\mu\nu} \tilde{W}^{\mu\nu} - \frac{g_3^2}{4\pi} \frac{1}{4\Lambda_3} s G_{\mu\nu} \tilde{G}^{\mu\nu} \end{aligned} \quad (2.2)$$

where \tilde{B} , \tilde{W} and \tilde{G} are the field strength duals, $\tilde{F}_{\mu\nu} = 1/2\epsilon_{\mu\nu\rho\sigma}F^{\rho\sigma}$. The collider phenomenology aspects of s we will focus on depend only mildly on its CP nature, unlike the DM properties of ψ .

The interpretation of the suppression mass scales in Eqs. (2.1) and (2.2) is heavily model-dependent. The most straightforward way of obtaining such interactions is, *e.g.*, by integrating out loops of heavy vector-like fermions. In our analysis the Λ couplings will be treated merely as a parametrisation of the underlying physics, without any detailed reference to their potential ultraviolet (UV) origins, and the parameter ranges we will choose to work with are mostly motivated by the requirements of satisfying the various experimental constraints on the resonance s and studying whether they can be reconciled. For the sake of illustration, in App. A we nevertheless comment on the type of physics that could lead to such couplings and point out some of the corresponding model-building challenges.

2.2 Collider implications and observational status

The Lagrangian (2.1) gives rise to a variety of collider signatures. The singlet s can be produced through gluon, vector boson fusion (VBF) or photon fusion and can decay into $g/\gamma/Z/W$ pairs, $Z\gamma$ and, if $m_\psi < m_s/2$, $\bar{\psi}\psi$ final states. We will focus on gluon fusion production, although VBF could provide extremely interesting distinct signatures.

The diphoton excess reported in [1, 2] appears at an invariant mass around 750 GeV, with a 3.6σ (2.0σ) and 2.6σ (1.2σ) local (global) significance for ATLAS and CMS respectively. A preliminary fit performed in [37] points, at 95% confidence level

¹For an earlier study of such interactions see, for example, [53].

(CL), to cross section values $\sigma(pp \rightarrow s) \times \text{BR}(s \rightarrow \gamma\gamma) \sim 1 - 5$ fb assuming a width $\Gamma_s = 5$ GeV and $\sigma(pp \rightarrow s) \times \text{BR}(s \rightarrow \gamma\gamma) \sim 2 - 12$ fb for a larger width $\Gamma_s = 40$ GeV when the ATLAS and CMS Run-1 and Run-2 results are combined.

One of the cleanest signatures of a new heavy scalar resonance described by the Lagrangian (2.1) would be a peak in the dijet or four-lepton invariant mass distributions. Currently the ATLAS and CMS collaborations do not provide dijet limits at $\sqrt{s} = 13$ TeV for masses as low as 750 GeV, as the presentation of their results starts at $m_s \sim 1$ TeV. The $\sqrt{s} = 8$ TeV ATLAS and CMS analyses presented in [54, 55] set a limit of $\sigma_{jj} < 1$ pb for a 1 TeV resonance coupling dominantly to gg (for a mass of 750 GeV the limit shown by ATLAS is of the order of 10 pb).

Passing to EW gauge boson final states, ATLAS sets the limits $\sigma_{ZZ} \lesssim 12$ fb [56] and $\sigma_{WW} \lesssim 40$ fb [57] for a 750 GeV particle decaying into ZZ/WW pairs. For the same mass the ATLAS search for a resonance decaying into a $Z\gamma$ final state places an upper bound of $\sigma_{\gamma Z} \leq 3.5$ fb [58], at a CM energy of 8 TeV. On the diphoton side, both ATLAS and CMS have presented upper bounds for the production cross section of a diphoton resonance at $\sqrt{s} = 8$ TeV, setting a limit $\sigma_{\gamma\gamma} \leq 2$ fb [59, 60].

2.3 Dark matter and a (pseudo-)scalar portal at 750 GeV

Another interesting possibility arising from the Lagrangian of Eq. (2.1) is that the fermion ψ could be responsible (also even partially) for the DM abundance observed in the Universe. It has already been shown that assuming standard thermal freeze-out the DM abundance observed by WMAP9 [61] and Planck [62] can indeed be obtained in this setup for a wide range of ψ masses [4, 5]. As reference values for the DM density, we consider the 3σ range from the (CMB+BAO+ H_0) WMAP 9-year results

$$\Omega h^2 = 0.1153 \pm 0.0057 . \quad (2.3)$$

The CP properties of s are crucial for the predicted relic density. In the CP -even case, the thermally averaged self-annihilation cross section $\langle\sigma v\rangle$ is velocity-suppressed, which amounts to large y_ψ coupling values being required in order to achieve the observed DM abundance. When s is odd under CP , this velocity suppression is lost and smaller values of y_ψ are sufficient to satisfy the bound (2.3). For reasonable values of Λ_3 , such that the 8 TeV LHC dijet bounds described in the previous paragraph are satisfied, the predicted relic abundance is found to be prohibitively large for $m_\psi \lesssim 200$ GeV in the CP -even case, and $m_\psi \lesssim 100$ GeV in the CP -odd one, unless non-perturbative values are considered for y_ψ .

Additional constraints come from direct detection (DD) and indirect detection (ID) experiments, with the predictions again depending strongly on the transformation properties of s under CP . DD constraints, and in particular the LUX [63] results, are relevant in the CP -even case. We find that, depending on the assumptions adopted for the quark (and, consequently, gluon) content of the nucleon, and

taking the couplings of s to the SM quarks to be identically zero, a lower limit can be set on the DM mass which ranges between ~ 200 and ~ 300 GeV. Some more details on our DD computations are given in App. B. ID constraints on the other hand are ineffective in the CP -even case, due to the velocity suppression in $\langle\sigma v\rangle$.

The situation is inverted when s is CP -odd. The Lagrangian (2.2) yields a negligible spin-independent scattering cross section off nuclei. Instead, in this case it is ID which becomes relevant. The strongest bounds come from the six-year Fermi satellite searches for DM annihilation-induced continuum gamma-rays from dwarf spheroidal galaxies [64] and for gamma-ray lines from the galactic centre [65]. Additional constraints could also arise from the AMS-02 searches for antiprotons [66] as extracted, for example, in [67], which we nonetheless find to be weaker for the DM mass range of our interest. A more detailed discussion of ID constraints and perspectives can be found in [68]. For low values of $\Lambda_{1,2} \lesssim 50$ GeV, the gamma-ray line searches dominate and can exclude DM masses up to ~ 200 GeV, depending also on the assumptions for the underlying DM halo profile in the Milky Way. Continuum gamma-ray searches give comparable but slightly weaker bounds.

For reasons of clarity, throughout the subsequent discussion we will ignore DM detection constraints. The indicative numbers quoted previously, although subject to uncertainties, show nonetheless that DD and ID could provide valuable information on scenarios relating the putative diphoton excess with DM.

3 Analysis

For our analysis, we calculate diphoton and dijet cross sections at the 13 TeV LHC, as well as monojet production for $\sqrt{s} = 8$ TeV, mediated by the s resonance as described by the Lagrangian (2.1). In particular we consider the processes:

$$\begin{aligned}
 pp &\rightarrow s \rightarrow \gamma\gamma, \\
 pp &\rightarrow s \rightarrow jj, \\
 pp &\rightarrow s \rightarrow \psi\psi j
 \end{aligned}
 \tag{3.1}$$

We moreover compute the relic abundance of ψ assuming standard thermal freeze-out.

3.1 Analysis setup

The model described in Eqs. (2.1) and (2.2) has been implemented in the UFO format [69] through the Feynrules package [70] and event samples have been generated through MadGraph5_aMC@NLO [71]. In particular, the 13 TeV $pp \rightarrow \gamma\gamma$ and $pp \rightarrow jj$ cross sections were computed at parton level and convoluted with the CTEQ6L1 [72]

parton distribution functions². Furthermore, we have also calculated the width of the resonance within the same set up. DM observables have been computed with the `micrOMEGAs4.1` package [73], with the exception of the spin-independent WIMP-nucleon scattering cross section, which has been calculated analytically as described in App. B.

In order to exploit the constraints arising from 8 TeV data on monojet signatures, we have used a recast version of the ATLAS monojet search ATLAS-SUSY-2013-21 [74]³, implemented in the `MadAnalysis5` [76] package and described on the Public Analysis Database (PAD) [77]. This recast analysis is publicly available online at [78], together with a validation note [79]. This analysis targeted decays of the SUSY partner of the top quark, the stop, into a charm quark and neutralino final state, for a compressed stop-neutralino spectrum. The search tags the emission of a hard initial state radiation jet recoiling against the E_T^{miss} .

The generated parton level events for the process $pp \rightarrow \psi\psi j$ were hadronised with the `PYTHIA6` [80] package. A merging scale of 30 GeV was used to perform the Matrix element-Parton Shower matching (ME-PS) [81] between the 0 and 1 jet samples. A fast detector simulation was performed with the `MadAnalysis5` tuned version of the `Delphes3` [82] package as described in [77]. Jets were reconstructed using `FastJet` [83], via an anti- k_T [84] algorithm with a cone size of 0.4 and they are required to have $p_T > 20$ GeV. Furthermore we have used the ATLAS AUET2B tune [85] to simulate underlying events.

The reconstructed events were finally passed through the aforementioned recast ATLAS monojet analysis [74], which consists of three signal regions targeting $(p_T^j, E_T^{\text{miss}})$ threshold combinations of (280, 200), (340, 340) and (450, 450) GeV respectively. To obtain the constraints arising from the ATLAS monojet analysis, we have used the `exclusion-CLs.py` module implemented in the `MadAnalysis5` package. This module determines, given the number of signal, expected and observed background events, together with the background uncertainty (the latter three directly taken from the experimental publications), the most sensitive signal region (SR) of the analysis and the exclusion CL using the CLs prescription [86, 87] for the most sensitive SR.

For our analysis we scanned over Λ_3 and y_ψ for discrete values of Λ_1, Λ_2 and DM masses m_ψ , setting $\Lambda_1 = \Lambda_2 \equiv \Lambda_{1,2}$ for simplicity. In particular the following parameter scan was performed⁴

²Given the preliminary nature of the excess seen in the early 13 TeV data, the main uncertainties do not come from the analysis setup but rather from the experimental side. In this respect these details are given for completeness and to render our analysis more transparent.

³Other dedicated DM searches for $j + E_T^{\text{miss}}$ final states exist and can also be used. These searches, e.g. [75], contain several signal regions corresponding to different $j + E_T^{\text{miss}}$ cuts. The cuts on the analysis used in this study are nonetheless comparable to the ones used in DM searches.

⁴Since the monojet analysis is expected to have a mild dependence on the CP properties of the

- $m_\psi = 50, 150, 250, 350$ and 450 GeV,
- $\Lambda_{1,2} = 20, 50, 200$ and 400 GeV,
- $\Lambda_3 \in [200, 3000]$ GeV and $y_\psi \in [0.05, 4\pi]$.

Note that we have chosen to study relatively extreme values for $\Lambda_{1,2}$, since the behaviour of the various observables in the intermediate regime can be inferred via an interpolation between the values we consider. We should also point out that especially for the $\Lambda_{1,2} = 20$ and 50 GeV scenarios, substantial cross sections into ZZ and WW final states are predicted over a significant fraction of the parameter space, which are in direct conflict with the corresponding limits quoted in Sec. 2.2. We have explicitly verified that all of our scenarios with $\sigma_{\gamma\gamma} < 12$ fb, *i.e.* within the region preferred by the observed diphoton excess, are consistent with the relevant bounds on $\sigma_{ZZ/WW}$. Throughout the subsequent discussion, although these bounds will be omitted for clarity, the reader should keep in mind that ZZ/WW searches are (at least) in tension with all parameter space regions characterised by $\sigma_{\gamma\gamma} \gtrsim 18$ fb. This tension can be relaxed, for example, by considering scenarios with $\Lambda_2 \gg \Lambda_1$.

3.2 Results

We first consider the regime where $m_\psi < m_s/2$. This region is particularly interesting as it can in principle account for the potentially large width of the resonance through decays into the invisible state ψ [4, 5]. Motivated by the comments on the DM density made in Sec. 2.3, we choose to present our results for the cases $m_\psi = 250$ and 350 GeV. For $m_\psi = 50$ GeV, it is simply impossible to reproduce the observed DM abundance for perturbative values of y_ψ . For $m_\psi = 150$ GeV, it is possible to do so in the CP -odd case but only at the cost of large values for y_ψ which amount to an exceedingly large width Γ_s (this regime is also in quite strong tension with indirect searches for gamma-ray lines). We will nonetheless comment on our findings for these cases later on.

Our main results are presented in Fig. 1 for $m_\psi = 250$ GeV and in Fig. 2 for $m_\psi = 350$ GeV, for the values $\Lambda_{1,2} = 20, 50, 200, 400$ GeV in the top left, top right, bottom left and bottom right panels respectively. The predicted 13 TeV production cross sections for the dijet (blue contours) and diphoton (red regions) final states are shown, along with the total width of the resonance (green contours). The 95% CL monojet constraints derived at 8 TeV from the recast search as described in Sec. 3.1 are also overlaid (black contours). Finally, where possible, a blue (green) band satisfying the DM bound (2.3) for the CP -even (CP -odd) case is shown. All cross sections are given in fb and masses/widths in GeV. Note that the results for extremely

mediator [88–90], for simplicity we have only performed our computations for the scalar case.

large widths should be interpreted with care. In this regime in fact a full momentum-dependent width ought to be used in the resonance propagator when performing the calculation.

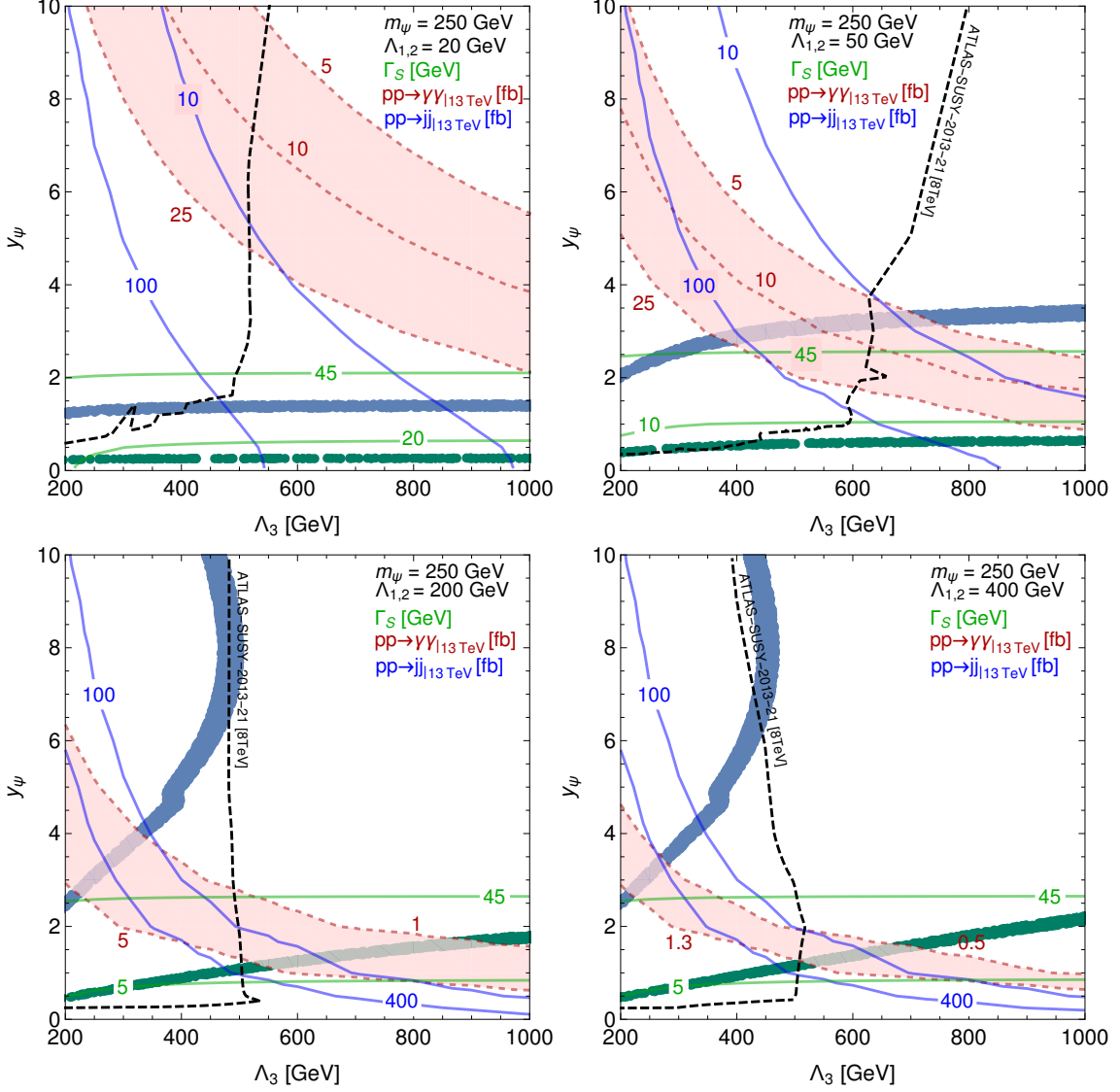


Figure 1. Predictions for $pp \rightarrow s \rightarrow \gamma\gamma$ (red band) and $pp \rightarrow s \rightarrow jj$ (blue contours) cross sections at $\sqrt{s} = 13$ TeV, overlaid with 8 TeV monojet constraints (black line) and the width of the resonance s (green contours). The mass of the invisible fermion ψ is fixed at $m_\psi = 250$ GeV and $\Lambda_{1,2} = 20, 50, 200, 400$ GeV in the top left, top right, bottom left and bottom right panels respectively. Monojet constraints are derived at 95% C.L. The blue (green) band shows regions of parameter space compatible with the observed DM density for a scalar (pseudoscalar) mediator.

A first observation that can be made is that in both the $m_\psi = 250$ GeV and

350 GeV cases, the width of the resonance is fairly independent of Λ_3 , especially when $\Gamma_s \gtrsim 10$ GeV. This behaviour can be understood from the fact that in most of the parameter space at hand, Γ_s is completely dominated by the invisible (and, to a lesser extent, EW gauge boson) contribution unless y_ψ and Λ_3 simultaneously attain small values. The dijet and diphoton cross sections, on the other hand, depend both on y_ψ and Λ_3 . The dijet cross sections are sizeable for smaller Λ_3 scales, due to the increase in the s production cross section, but also for smaller values of y_ψ . A similar behaviour is present in the diphoton cross section which moreover increases, as expected, with decreasing $\Lambda_{1,2}$. The y_ψ dependence of the two cross sections is due to both the increase in $\text{BR}(s \rightarrow gg/\gamma\gamma)$ and to the decrease of the total width of the resonance. In order to get a feeling of the impact that dijet searches could have on our parameter space, we can naively extrapolate the existing 13 TeV constraints presented in [91, 92] for a minimal resonance mass of 1.5 TeV down to 750 GeV, assuming that the limit remains constant. Such a – very aggressive – extrapolation would amount to a limit of the order of a few pb, which could be strong enough to probe part of the $m_\psi = 350$ GeV scenario of Fig. 2. However, a dedicated experimental study is required in order to make any concrete statement.

Leaving monojet constraints aside for the moment, we see that in the $m_\psi = 250$ GeV case (Fig. 1) the requirements for a substantial diphoton cross section and a large resonance width $\Gamma_s > 20$ GeV can be reconciled in substantial parts of the parameter space, except for the case $\Lambda_{1,2} = 400$ GeV where the predicted diphoton cross section is too low. The relic abundance constraint for ψ significantly reduces the available parameter space, although it is still possible to accommodate all three requirements assuming a CP -even scalar for $\Lambda_{1,2} = 20$ or 50 GeV (the latter at the price of a slightly larger width) and a CP -odd scalar when $\Lambda_{1,2} = 200$ GeV. Note that DM is underabundant (overabundant) above (below) the blue and green bands. The imposition of the monojet constraints has an important impact on the parameter space, excluding Λ_3 values below ~ 500 GeV regardless of the value of y_ψ , unless $y_\psi \lesssim 0.25$. This behaviour can be understood by the fact that for sufficiently large values of y_ψ , the branching ratio into ψ pairs is basically unity and the monojet cross section essentially only depends on Λ_3 , except for its dependence on the total width of s . The only surviving region for the parameter choices shown in Fig. 1 where all requirements can be (approximately) reconciled is for $\Lambda_{1,2} = 200$ GeV, a CP -odd scalar s and $\Lambda_3 \gtrsim 500$ GeV. Interestingly, though, by comparing the $\Lambda_{1,2} = 20$ and 50 GeV cases, we can deduce that all requirements can also be rendered compatible assuming a CP -even scalar for $\Lambda_{1,2}$ values around 30 GeV and for Λ_3 values above the monojet exclusion bounds. Besides, if the relic abundance requirement is dropped, then for sufficiently large Λ_3 values the low $\Lambda_{1,2}$ scenarios can generically account for a broad resonance with a large enough diphoton cross section.

We now turn our attention to Fig. 2, which corresponds to $m_\psi = 350$ GeV. In this case, the reduction of phase space for the $s \rightarrow \psi\psi$ decay generically leads

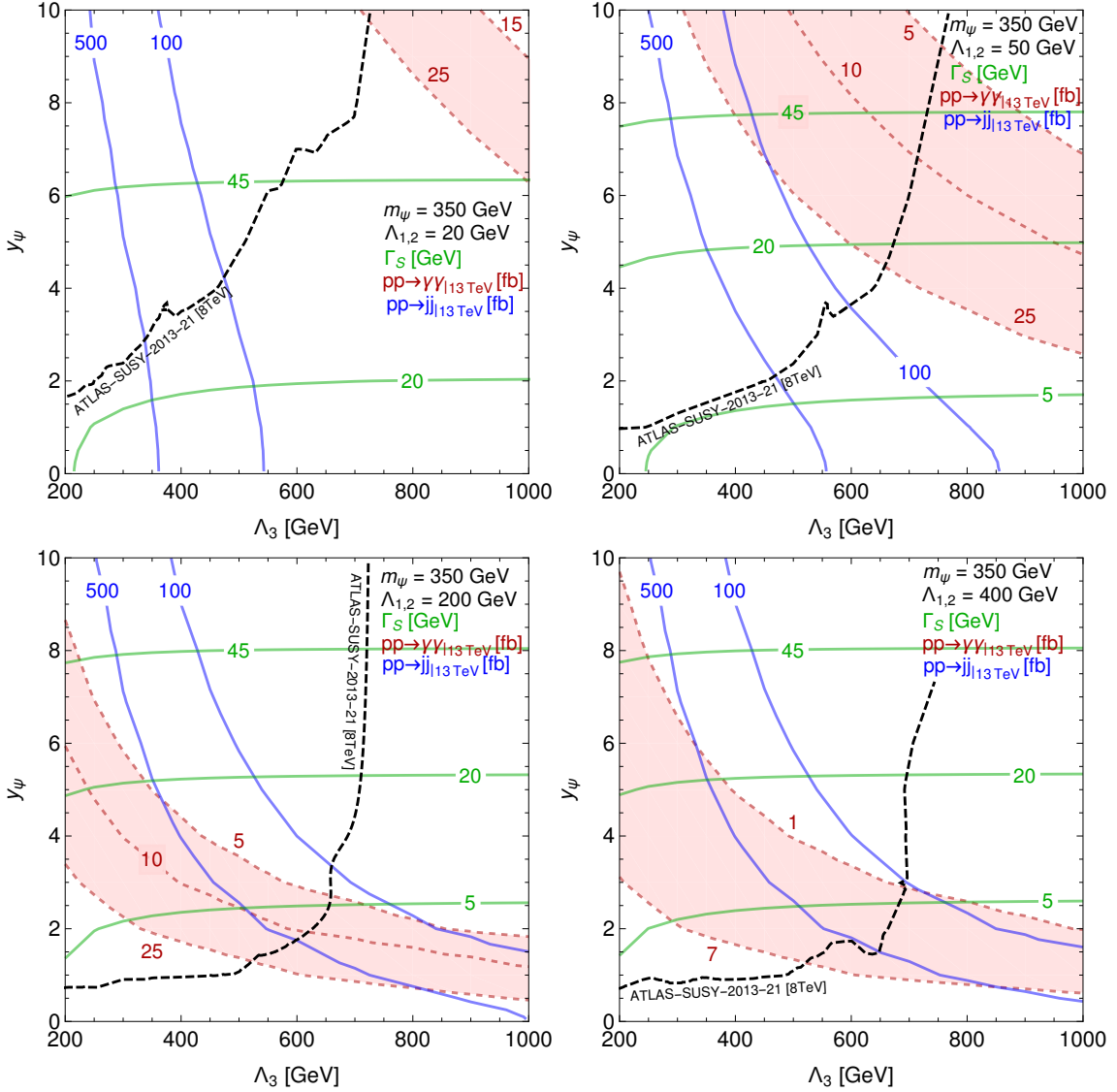


Figure 2. Predictions for $pp \rightarrow s \rightarrow \gamma\gamma$ (red band) and $pp \rightarrow s \rightarrow jj$ (blue contours) cross sections at $\sqrt{s} = 13$ TeV, overlaid with 8 TeV monojet constraints (black line) and the width of the resonance s (green contours). The mass of the invisible fermion ψ is fixed at $m_\psi = 350$ GeV and $\Lambda_{1,2} = 20, 50, 200, 400$ GeV in the top left, top right, bottom left and bottom right panels respectively. Monojet constraints are derived at 95% C.L. The DM abundance can be reproduced for very low y_ψ values of ~ 0.07 and ~ 0.02 in the scalar and pseudoscalar cases respectively and the corresponding points are omitted for clarity.

to smaller widths and, consequently, larger diphoton (and dijet) cross sections with respect to the $m_\psi = 250$ GeV scenario. The monojet constraint shown again as a black line rules out most of the parameter space with $\Lambda_3 \lesssim 650$ GeV. For this value of m_ψ the observed relic density is obtained for $y_\psi \sim 0.07$ (0.02) for the CP -even (CP -odd) case which lies at the lower edge of our plots and the corresponding points

are not shown. The relic density constraint is fully incompatible with a large width but can be reconciled with the diphoton excess for sufficiently large $\Lambda_{1,2,3}$ values. Conversely, when DM constraints are dismissed, a substantial diphoton cross section is compatible with a large invisible width for sufficiently low $\Lambda_{1,2}$ values.

A comparison of the excluded regions for ψ masses of 250 and 350 GeV from the monojet searches shows that for large values of y_ψ , the limits are stronger in the latter case. This is due to a reduction of the total width as m_ψ increases, leading to an enhancement of the total cross section. However for small values of y_ψ , where the total width is sufficiently small in both scenarios, the exclusion is stronger for the 250 case as compared to 350 due to the higher kinematic acceptance of the monojet search for smaller ψ masses.

The regime between $m_\psi = 250$ and 350 GeV can be understood as an interpolation between the results presented in Figs. 1 and 2. Indeed, for such intermediate masses we expect that it is still possible to reconcile a broad diphoton resonance s with the correct DM relic density assuming a CP -even scalar s . This should happen in particular for relatively low values of $\Lambda_{1,2} \sim 20 - 50$ GeV. Referring for example to the top right panel of Fig.1, increasing m_ψ would amount to smaller values of the y_ψ coupling being required in order to reproduce the observed relic abundance as the “funnel region” is gradually approached. Schematically, the blue band would then move downwards, towards larger diphoton cross sections and more reasonable Γ_s values of the order of 10 to 45 GeV.

In the case $m_\psi < 250$ GeV, on the other hand, the opposite behaviour is expected. For slightly smaller ψ masses (but larger than 150 GeV according to our findings), it is now the CP -odd case which can be relevant. Referring again to the top right panel of Fig. 1, decreasing m_ψ would amount to larger values of the y_ψ coupling being required in order to achieve the correct relic density. The green band would then move upwards and become compatible with the width and diphoton cross section requirements. Besides, we remind the reader that such a configuration could face severe problems with gamma-ray line searches.

Given the extremely preliminary nature of the diphoton excess, we have no a priori reason to consider only large width scenarios. Therefore, we also consider two examples with $2m_\psi > m_s$, necessarily leading to a narrow width for the resonance s . In this case the invisible final state is therefore produced via an off-shell mediator. In Fig. 3, we present the results for $m_\psi = 450$ GeV with scale choices of $\Lambda_{1,2} = 300$ and 500 GeV (left and right panel respectively). As illustrated in Figs. 1 and 2, the LHC monojet cross sections do not depend drastically on the scale $\Lambda_{1,2}$, hence we derived the constraints for $\Lambda_{1,2} = 500$ GeV, and have used them for the $\Lambda_{1,2} = 300$ GeV case as well. The expected diphoton cross sections in this case can easily exceed 10 fb, the width of the resonance is smaller, and the monojet search excludes a much smaller region of parameter space, as is expected. The relic density band, once again shown in blue (green) for the CP -even (CP -odd) case, passes very well through the

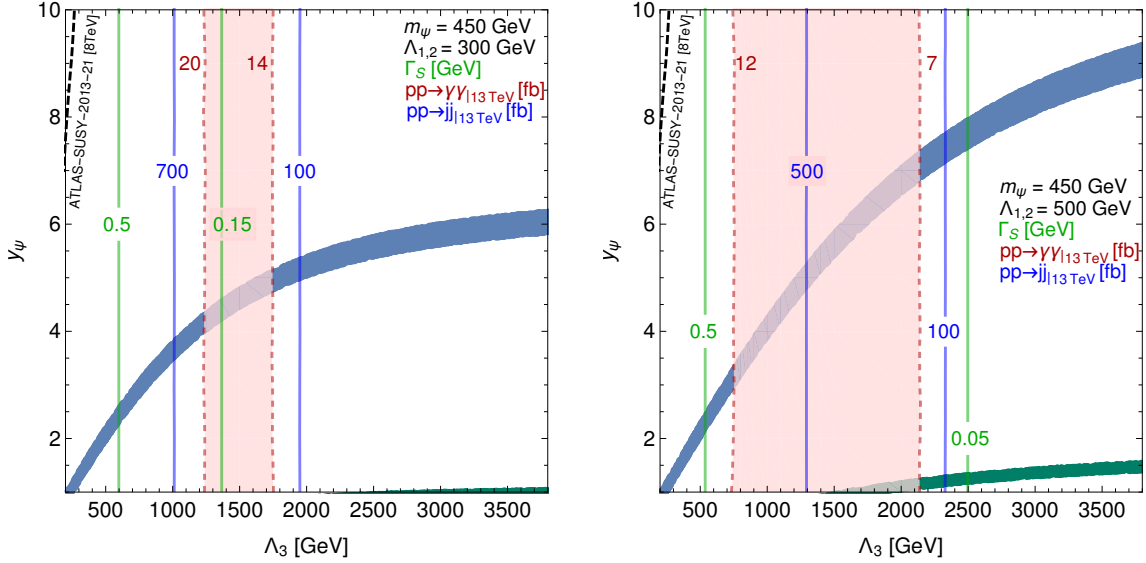


Figure 3. Predictions for $pp \rightarrow s \rightarrow \gamma\gamma$ (red band) and $pp \rightarrow s \rightarrow jj$ (blue contours) cross sections at $\sqrt{s} = 13$ TeV, overlaid with 8 TeV monojet constraints (black line) and the width of the resonance s (green contours). The mass of the invisible fermion ψ is fixed at $m_\psi = 450$ GeV and $\Lambda_{1,2} = 300, 500$ GeV in the left and right panel respectively. Monojet constraints are derived at 95% C.L. The blue (green) band shows regions of parameter space compatible with the observed DM density for a scalar (pseudoscalar) mediator.

regions of preferred parameter space and one can obtain the correct DM abundance while within the LHC bounds.

4 Summary and conclusions

Motivated by the recent hint of a possibly broad excess in the diphoton channel at the LHC, in this work we studied monojet constraints on potential invisible decays of a scalar particle with a mass of ~ 750 GeV. We examined the extent to which it is possible to reconcile these constraints with the preferred diphoton cross section values, a large resonance width and, eventually, the relic DM abundance in the Universe in case the invisible decay product is stable on cosmological timescales. We have also presented predictions for the dijet production cross section at the 13 TeV LHC.

We showed that monojet searches already place important constraints on interpretations of the putative 750 GeV diphoton resonance as a portal to a DM sector. Nevertheless for limited regions of the parameter space it is still possible to accommodate all requirements. These regions will be probed, assuming the diphoton excess persists in the LHC data, in the next few years from a combination of LHC analyses and direct/indirect DM detection searches.

Once either the DM or the large width requirements are dropped, it is much easier to reconcile the remaining conditions. Concretely, a broad resonance can still be explained through invisible decays without conflicting monojet searches, whereas a narrow resonance can easily mediate the DM-SM interactions. Additional interesting signatures not considered in this work include multijets (along the lines of [93]), γZ and four- or two-lepton final states as well as, in the case of strong coupling to EW gauge bosons, VBF production of the resonance.

In any case, within the next few months it will become clear whether the 750 GeV “excess” constitutes merely a statistical fluctuation or a sign of – long sought for – physics beyond the Standard Model.

5 Acknowledgements

AG and SK are supported by the ‘New Frontiers’ program of the Austrian Academy of Sciences. The work of DS is supported by the French ANR, project DMAstroLHC, ANR-12-BS05-0006, and by the Investissements d’avenir, Labex ENIGMASS. We thank Giorgio Arcadi, Yann Mambrini and Alberto Mariotti for several useful discussions.

A Some comments on potential UV completions

In order to get a feeling of the type of NP that could give rise to interactions like the ones described by the Lagrangians of Eqs. (2.1) and (2.2) and the corresponding values of $\Lambda_{1,2,3}$ used in the analysis, we assume a set of additional vector-like fermions f charged under the SM gauge group that couple to s through Yukawa-type terms.

Fermions transforming according to the fundamental representation of $SU(3)_c$ will generate a partial width $\Gamma(s \rightarrow gg)$ as [94, 95]

$$\Gamma_{\text{UV}}(s \rightarrow gg) = \frac{\alpha_s^2 m_s^3}{72\pi^3} \left| \frac{3}{4} \sum_f \frac{y_f}{m_f} F_{1/2}^{s\pm}(\tau_f) \right|^2 \quad (\text{A.1})$$

where α_s is the strong coupling constant, m_s the resonance mass, y_f and m_f the Yukawa couplings and masses of the heavy fermions and $F_{1/2}^{s\pm}(\tau)$ the loop form factor for the CP even and CP odd case respectively, which reads

$$F_{1/2}^{s+}(\tau_f) = \frac{2}{\tau_f^2} [\tau_f + (\tau_f - 1)f(\tau_f)] \quad (\text{A.2})$$

$$F_{1/2}^{s-}(\tau_f) = 2\tau_f^{-1} f(\tau_f) \quad (\text{A.3})$$

with $\tau_f \equiv m_s^2/(4m_f^2)$. For heavy coloured fermions, that is assuming $\tau_f \leq 1$, the function $f(\tau_f)$ is given by

$$f(\tau_f) = \arcsin^2 \sqrt{\tau_f}, \quad \tau_f \leq 1. \quad (\text{A.4})$$

The corresponding expression for $\Gamma(s \rightarrow gg)$ obtained from the Lagrangians of Eqs. (2.1) and (2.2), on the other hand, reads

$$\Gamma_{\text{EFT}}(s \rightarrow gg) = \frac{\alpha_s^2 m_s^3}{8\pi \Lambda_3^2}. \quad (\text{A.5})$$

Then, by matching the two expressions we can obtain the value of Λ_3 as a function of the fermion masses, their Yukawa couplings and their multiplicities. Assuming for simplicity that all fermions couple identically to s and that there are N_f copies of them, we get

$$\Lambda_3 = 3\pi \frac{m_f}{N_f y_f} \frac{4}{3} \frac{1}{|F_{1/2}^{s\pm}(\tau_f)|}. \quad (\text{A.6})$$

When $m_f \gtrsim m_s$, the form factor F becomes $|F_{1/2}^{s+}(\tau_f)| \simeq 4/3$ for a CP-even s and $|F_{1/2}^{s-}(\tau_f)| \simeq 2$ for a CP-odd one. We can then write

$$\Lambda_3 = \begin{cases} \frac{3\pi m_f}{N_f y_f} & (\text{scalar}) \\ \frac{2\pi m_f}{N_f y_f} & (\text{pseudoscalar}). \end{cases} \quad (\text{A.7})$$

If we assume coloured fermions with a mass of 1 TeV, a value compatible with the latest experimental limits on heavy quark masses ⁵ [96], for $N_f = 1$ and $y_f = 1$, Eq. (A.7) leads to a large value for the scale $\Lambda_3 \gtrsim 6$ TeV. Lower values, down to ~ 400 GeV, can be obtained assuming higher fermion multiplicities and/or larger couplings to the resonance s . For example for $N_f = y_f = 5$ we obtain $\Lambda_3 = 400$ GeV and 250 GeV for the CP even and CP odd case respectively.

Similarly, in the EW sector the decay width $\Gamma(s \rightarrow \gamma\gamma)$, assuming the process is mediated by loops of fermions f , reads [95]

$$\Gamma_{\text{UV}}(s \rightarrow \gamma\gamma) = \frac{\alpha^2 m_s^3}{256\pi^3} \left| \sum_f N_f^c Q_f^2 \frac{y_f}{m_f} F_{1/2}^{s\pm}(\tau_f) \right|^2 \quad (\text{A.8})$$

where all the factors follow from Eq. (A.1) apart from the fine structure constant α , the color factor N_f^c and the electric charges of the fermions running in the loop, Q_f . In our effective description, taking $\Lambda_1 = \Lambda_2 \equiv \Lambda_{1,2}$, the corresponding expression becomes

$$\Gamma_{\text{EFT}}(s \rightarrow \gamma\gamma) = \frac{\alpha^2 m_s^3}{16\pi \Lambda_{1,2}^2}. \quad (\text{A.9})$$

⁵For a consistent UV completion it is important to mention the necessity to decay these NP states. This can be achieved by introducing a linear mixing between the heavy quarks and the SM fermions, for example the top quark. While this introduces a certain degree of model dependence in the discussion, we assume this mixing to be small enough so that the $s f \bar{f}$ interaction does not cause a large $s \rightarrow t \bar{t}$ decay rate, while leaving the previous discussion on the loop induced ggs coupling unaffected.

We can then establish the correspondence

$$\Lambda_{1,2} = \frac{4\pi m_f}{N_f Q_f^2 y_f |F_{1/2}^{s\pm}(\tau_f)|} \quad (\text{A.10})$$

The form factor F attains its maximal value close to the threshold $m_f \sim m_s/2$ (note that one has to consider $m_f \gtrsim m_s/2$ so as to avoid the tree level decay of s into a pair of heavy fermions). The explicit value is $|F_{1/2}^{s+}(\tau_f)| \simeq 2$ and $|F_{1/2}^{s-}(\tau_f)| \simeq 5$ for the CP-even and CP-odd cases respectively. Taking then $m_f \sim m_s/2$ and assuming the heavy fermions to be neutral under $SU(3)_c$ and, again for simplicity, to all couple identically to s we obtain

$$\Lambda_{1,2} \sim \begin{cases} \frac{2350 \text{ GeV}}{(N_f Q_f^2 y_f)} & \text{scalar.} \\ \frac{950 \text{ GeV}}{(N_f Q_f^2 y_f)} & \text{pseudoscalar.} \end{cases} \quad (\text{A.11})$$

It is then clear that, at least for $Q_f = 1$, achieving the lowest $\Lambda_{1,2}$ scales we consider in our analysis (20 GeV) is quite difficult in such a picture involving vector-like fermions, for both the cases of a CP even or CP odd scalar, even if the perturbativity limits are saturated for each fermion. Note, however, that $\Lambda_{1,2}$ needs not be interpreted as coming from such a type of UV completion but could instead parametrize some appropriate strong dynamics. Besides, for the higher values of $\Lambda_{1,2}$ considered in our analysis perturbative embeddings of the Lagrangians (2.1) and (2.2) can be envisaged fairly easily. For example, taking again $N_f = y_f = 5$, we obtain $\Lambda_{1,2} = 100$ and 40 GeV for the CP even and CP odd case respectively. Note that even if the theory is perturbative at the input scale, renormalization group evolution of the couplings may lead to the apparition of Landau poles at scales of a few TeV. A discussion of such effects can be found in [10].

B Some more details on direct detection

For convenience, we recall here the formalism relevant to the computation of the DM-nucleon spin-independent scattering cross section, following closely Ref. [97]. Integrating out the scalar s in Eq. (2.1), we obtain an effective coupling of ψ pairs to gluons described, to lowest order, by the Lagrangian

$$\mathcal{L}_{\text{eff}} = f_G \bar{\psi} \psi G_{\mu\nu} G^{\mu\nu} \quad (\text{B.1})$$

where in our conventions the coefficient f_G is given by

$$f_G \equiv \frac{y_\psi}{2} \frac{\alpha_s}{4\Lambda_3} \frac{1}{m_s^2}. \quad (\text{B.2})$$

The spin-independent scattering cross section is then simply computed by

$$\sigma_{\text{SI}} = \frac{4}{\pi} \mu_{\psi N}^2 |f_p|^2 \quad (\text{B.3})$$

where the amplitude f_p reads

$$f_p = m_p \frac{8\pi}{9\alpha_s} f_G f_{TG} \quad (\text{B.4})$$

and f_{TG} is the gluon form-factor. The latter can be related to the standard f_{Tq} quantities that describe the “quark content” of the nucleon, $f_{TG} = 1 - \sum_{q=u,d,s} f_{Tq}$. The constraints quoted in Sec. 2.3 are based on the choice $f_{Tu} = 0.0153$, $f_{Td} = 0.0191$ and $f_{Ts} = 0.0447$ (which is also the default choice in the public code `micrOMEGAs`).

It should be noted that the cross section depends quite strongly on the choices for the f_{Tq} quantities. For example, older computations of σ_{SI} used a much larger value for f_{Ts} , which would decrease the predicted cross section. All recent lattice simulations point to values close to the ones we have used. Furthermore, the spin-independent cross section changes quite drastically once couplings to quarks are turned on. In particular, as also pointed out in [4], couplings to heavy quarks tend to cancel out the gluon contribution. It is then clear that the behaviour of σ_{SI} in a UV-complete model could indeed be fairly different than the one predicted by the Lagrangian (2.1).

References

- [1] *Search for resonances decaying to photon pairs in 3.2 fb⁻¹ of pp collisions at $\sqrt{s} = 13$ TeV with the ATLAS detector*, Tech. Rep. ATLAS-CONF-2015-081, CERN, Geneva, Dec, 2015.
- [2] **CMS Collaboration** Collaboration, *Search for new physics in high mass diphoton events in proton-proton collisions at $\sqrt{s} = 13$ TeV*, Tech. Rep. CMS-PAS-EXO-15-004, CERN, Geneva, 2015.
- [3] K. Harigaya and Y. Nomura, *Composite Models for the 750 GeV Diphoton Excess*, [arXiv:1512.04850](#).
- [4] Y. Mambrini, G. Arcadi, and A. Djouadi, *The LHC diphoton resonance and dark matter*, [arXiv:1512.04913](#).
- [5] M. Backovic, A. Mariotti, and D. Redigolo, *Di-photon excess illuminates Dark Matter*, [arXiv:1512.04917](#).
- [6] A. Angelescu, A. Djouadi, and G. Moreau, *Scenarii for interpretations of the LHC diphoton excess: two Higgs doublets and vector-like quarks and leptons*, [arXiv:1512.04921](#).
- [7] S. Knapen, T. Melia, M. Papucci, and K. Zurek, *Rays of light from the LHC*, [arXiv:1512.04928](#).

- [8] D. Buttazzo, A. Greljo, and D. Marzocca, *Knocking on New Physics' door with a Scalar Resonance*, [arXiv:1512.04929](#).
- [9] A. Pilaftsis, *Diphoton Signatures from Heavy Axion Decays at LHC*, [arXiv:1512.04931](#).
- [10] R. Franceschini, G. F. Giudice, J. F. Kamenik, M. McCullough, A. Pomarol, R. Rattazzi, M. Redi, F. Riva, A. Strumia, and R. Torre, *What is the gamma gamma resonance at 750 GeV?*, [arXiv:1512.04933](#).
- [11] S. Di Chiara, L. Marzola, and M. Raidal, *First interpretation of the 750 GeV di-photon resonance at the LHC*, [arXiv:1512.04939](#).
- [12] T. Higaki, K. S. Jeong, N. Kitajima, and F. Takahashi, *The QCD Axion from Aligned Axions and Diphoton Excess*, [arXiv:1512.05295](#).
- [13] S. D. McDermott, P. Meade, and H. Ramani, *Singlet Scalar Resonances and the Diphoton Excess*, [arXiv:1512.05326](#).
- [14] J. Ellis, S. A. R. Ellis, J. Quevillon, V. Sanz, and T. You, *On the Interpretation of a Possible ~ 750 GeV Particle Decaying into $\gamma\gamma$* , [arXiv:1512.05327](#).
- [15] M. Low, A. Tesi, and L.-T. Wang, *A pseudoscalar decaying to photon pairs in the early LHC run 2 data*, [arXiv:1512.05328](#).
- [16] B. Bellazzini, R. Franceschini, F. Sala, and J. Serra, *Goldstones in Diphotons*, [arXiv:1512.05330](#).
- [17] R. S. Gupta, S. Jger, Y. Kats, G. Perez, and E. Stamou, *Interpreting a 750 GeV Diphoton Resonance*, [arXiv:1512.05332](#).
- [18] C. Petersson and R. Torre, *The 750 GeV diphoton excess from the goldstino superpartner*, [arXiv:1512.05333](#).
- [19] E. Molinaro, F. Sannino, and N. Vignaroli, *Strong dynamics or axion origin of the diphoton excess*, [arXiv:1512.05334](#).
- [20] B. Dutta, Y. Gao, T. Ghosh, I. Gogoladze, and T. Li, *Interpretation of the diphoton excess at CMS and ATLAS*, [arXiv:1512.05439](#).
- [21] Q.-H. Cao, Y. Liu, K.-P. Xie, B. Yan, and D.-M. Zhang, *A Boost Test of Anomalous Diphoton Resonance at the LHC*, [arXiv:1512.05542](#).
- [22] S. Matsuzaki and K. Yamawaki, *750 GeV Diphoton Signal from One-Family Walking Technipion*, [arXiv:1512.05564](#).
- [23] A. Kobakhidze, F. Wang, L. Wu, J. M. Yang, and M. Zhang, *LHC diphoton excess explained as a heavy scalar in top-seesaw model*, [arXiv:1512.05585](#).
- [24] R. Martinez, F. Ochoa, and C. F. Sierra, *Diphoton decay for a 750 GeV scalar dark matter*, [arXiv:1512.05617](#).
- [25] P. Cox, A. D. Medina, T. S. Ray, and A. Spray, *Diphoton Excess at 750 GeV from a Radion in the Bulk-Higgs Scenario*, [arXiv:1512.05618](#).

- [26] D. Becirevic, E. Bertuzzo, O. Sumensari, and R. Z. Funchal, *Can the new resonance at LHC be a CP-Odd Higgs boson?*, [arXiv:1512.05623](#).
- [27] J. M. No, V. Sanz, and J. Setford, *See-Saw Composite Higgses at the LHC: Linking Naturalness to the 750 GeV Di-Photon Resonance*, [arXiv:1512.05700](#).
- [28] S. V. Demidov and D. S. Gorbunov, *On sgoldstino interpretation of the diphoton excess*, [arXiv:1512.05723](#).
- [29] W. Chao, R. Huo, and J.-H. Yu, *The Minimal Scalar-Stealth Top Interpretation of the Diphoton Excess*, [arXiv:1512.05738](#).
- [30] S. Fichet, G. von Gersdorff, and C. Royon, *Scattering Light by Light at 750 GeV at the LHC*, [arXiv:1512.05751](#).
- [31] D. Curtin and C. B. Verhaaren, *Quirky Explanations for the Diphoton Excess*, [arXiv:1512.05753](#).
- [32] L. Bian, N. Chen, D. Liu, and J. Shu, *A hidden confining world on the 750 GeV diphoton excess*, [arXiv:1512.05759](#).
- [33] J. Chakraborty, A. Choudhury, P. Ghosh, S. Mondal, and T. Srivastava, *Di-photon resonance around 750 GeV: shedding light on the theory underneath*, [arXiv:1512.05767](#).
- [34] A. Ahmed, B. M. Dillon, B. Grzadkowski, J. F. Gunion, and Y. Jiang, *Higgs-radion interpretation of 750 GeV di-photon excess at the LHC*, [arXiv:1512.05771](#).
- [35] P. Agrawal, J. Fan, B. Heidenreich, M. Reece, and M. Strassler, *Experimental Considerations Motivated by the Diphoton Excess at the LHC*, [arXiv:1512.05775](#).
- [36] C. Csaki, J. Hubisz, and J. Terning, *The Minimal Model of a Diphoton Resonance: Production without Gluon Couplings*, [arXiv:1512.05776](#).
- [37] A. Falkowski, O. Slone, and T. Volansky, *Phenomenology of a 750 GeV Singlet*, [arXiv:1512.05777](#).
- [38] D. Aloni, K. Blum, A. Dery, A. Efrati, and Y. Nir, *On a possible large width 750 GeV diphoton resonance at ATLAS and CMS*, [arXiv:1512.05778](#).
- [39] Y. Bai, J. Berger, and R. Lu, *A 750 GeV Dark Pion: Cousin of a Dark G-parity-odd WIMP*, [arXiv:1512.05779](#).
- [40] E. Gabrielli, K. Kannike, B. Mele, M. Raidal, C. Spethmann, and H. Veerme, *A SUSY Inspired Simplified Model for the 750 GeV Diphoton Excess*, [arXiv:1512.05961](#).
- [41] R. Benbrik, C.-H. Chen, and T. Nomura, *Higgs singlet as a diphoton resonance in a vector-like quark model*, [arXiv:1512.06028](#).
- [42] J. S. Kim, J. Reuter, K. Rolbiecki, and R. R. de Austri, *A resonance without resonance: scrutinizing the diphoton excess at 750 GeV*, [arXiv:1512.06083](#).
- [43] A. Alves, A. G. Dias, and K. Sinha, *The 750 GeV S-cion: Where else should we look for it?*, [arXiv:1512.06091](#).

- [44] E. Megias, O. Pujolas, and M. Quiros, *On dilatons and the LHC diphoton excess*, [arXiv:1512.06106](#).
- [45] L. M. Carpenter, R. Colburn, and J. Goodman, *Supersoft SUSY Models and the 750 GeV Diphoton Excess, Beyond Effective Operators*, [arXiv:1512.06107](#).
- [46] J. Bernon and C. Smith, *Could the width of the diphoton anomaly signal a three-body decay ?*, [arXiv:1512.06113](#).
- [47] M. Chala, M. Duerr, F. Kahlhoefer, and K. Schmidt-Hoberg, *Tricking Landau-Yang: How to obtain the diphoton excess from a vector resonance*, [arXiv:1512.06833](#).
- [48] X.-F. Han and L. Wang, *Implication of the 750 GeV diphoton resonance on two-Higgs-doublet model and its extensions with Higgs field*, [arXiv:1512.06587](#).
- [49] C. W. Murphy, *Vector Leptoquarks and the 750 GeV Diphoton Resonance at the LHC*, [arXiv:1512.06976](#).
- [50] L. D. Landau, *On the angular momentum of a system of two photons*, *Dokl. Akad. Nauk Ser. Fiz.* **60** (1948), no. 2 207–209.
- [51] C.-N. Yang, *Selection Rules for the Dematerialization of a Particle Into Two Photons*, *Phys. Rev.* **77** (1950) 242–245.
- [52] B. Patt and F. Wilczek, *Higgs-field portal into hidden sectors*, [hep-ph/0605188](#).
- [53] J. Jaeckel, M. Jankowiak, and M. Spannowsky, *LHC probes the hidden sector*, *Phys. Dark Univ.* **2** (2013) 111–117, [[arXiv:1212.3620](#)].
- [54] **CMS** Collaboration, V. Khachatryan et al., *Search for resonances and quantum black holes using dijet mass spectra in proton-proton collisions at $\sqrt{s} = 8$ TeV*, *Phys. Rev.* **D91** (2015), no. 5 052009, [[arXiv:1501.04198](#)].
- [55] **ATLAS** Collaboration, G. Aad et al., *Search for new phenomena in the dijet mass distribution using $p - p$ collision data at $\sqrt{s} = 8$ TeV with the ATLAS detector*, *Phys. Rev.* **D91** (2015), no. 5 052007, [[arXiv:1407.1376](#)].
- [56] **ATLAS** Collaboration, G. Aad et al., *Search for an additional, heavy Higgs boson in the $H \rightarrow ZZ$ decay channel at $\sqrt{s} = 8$ TeV in pp collision data with the ATLAS detector*, [arXiv:1507.05930](#).
- [57] **ATLAS** Collaboration, G. Aad et al., *Search for a high-mass Higgs boson decaying to a W boson pair in pp collisions at $\sqrt{s} = 8$ TeV with the ATLAS detector*, [arXiv:1509.00389](#).
- [58] **ATLAS** Collaboration, G. Aad et al., *Search for new resonances in $W\gamma$ and $Z\gamma$ final states in pp collisions at $\sqrt{s} = 8$ TeV with the ATLAS detector*, *Phys. Lett.* **B738** (2014) 428–447, [[arXiv:1407.8150](#)].
- [59] **CMS** Collaboration, V. Khachatryan et al., *Search for diphoton resonances in the mass range from 150 to 850 GeV in pp collisions at $\sqrt{s} = 8$ TeV*, *Phys. Lett.* **B750** (2015) 494–519, [[arXiv:1506.02301](#)].

- [60] **ATLAS** Collaboration, G. Aad et al., *Search for high-mass diphoton resonances in pp collisions at $\sqrt{s} = 8$ TeV with the ATLAS detector*, *Phys. Rev.* **D92** (2015), no. 3 032004, [[arXiv:1504.05511](#)].
- [61] **WMAP** Collaboration, G. Hinshaw et al., *Nine-Year Wilkinson Microwave Anisotropy Probe (WMAP) Observations: Cosmological Parameter Results*, *Astrophys. J. Suppl.* **208** (2013) 19, [[arXiv:1212.5226](#)].
- [62] **Planck** Collaboration, P. A. R. Ade et al., *Planck 2013 results. XVI. Cosmological parameters*, *Astron. Astrophys.* **571** (2014) A16, [[arXiv:1303.5076](#)].
- [63] **LUX** Collaboration, D. S. Akerib et al., *First results from the LUX dark matter experiment at the Sanford Underground Research Facility*, *Phys. Rev. Lett.* **112** (2014) 091303, [[arXiv:1310.8214](#)].
- [64] **Fermi-LAT** Collaboration, M. Ackermann et al., *Searching for Dark Matter Annihilation from Milky Way Dwarf Spheroidal Galaxies with Six Years of Fermi Large Area Telescope Data*, *Phys. Rev. Lett.* **115** (2015), no. 23 231301, [[arXiv:1503.02641](#)].
- [65] **Fermi-LAT** Collaboration, M. Ackermann et al., *Updated search for spectral lines from Galactic dark matter interactions with pass 8 data from the Fermi Large Area Telescope*, *Phys. Rev.* **D91** (2015), no. 12 122002, [[arXiv:1506.00013](#)].
- [66] <http://indico.cern.ch/event/381134/>.
- [67] G. Giesen, M. Boudaud, Y. Génolini, V. Poulin, M. Cirelli, P. Salati, and P. D. Serpico, *AMS-02 antiprotons, at last! Secondary astrophysical component and immediate implications for Dark Matter*, *JCAP* **1509** (2015), no. 09 023, [[arXiv:1504.04276](#)].
- [68] J.-C. Park and S. C. Park, *Indirect signature of dark matter with the diphoton resonance at 750 GeV*, [arXiv:1512.08117](#).
- [69] C. Degrande, C. Duhr, B. Fuks, D. Grellscheid, O. Mattelaer, and T. Reiter, *UFO - The Universal FeynRules Output*, *Comput. Phys. Commun.* **183** (2012) 1201–1214, [[arXiv:1108.2040](#)].
- [70] A. Alloul, N. D. Christensen, C. Degrande, C. Duhr, and B. Fuks, *FeynRules 2.0 - A complete toolbox for tree-level phenomenology*, *Comput. Phys. Commun.* **185** (2014) 2250–2300, [[arXiv:1310.1921](#)].
- [71] J. Alwall, R. Frederix, S. Frixione, V. Hirschi, F. Maltoni, O. Mattelaer, H. S. Shao, T. Stelzer, P. Torrielli, and M. Zaro, *The automated computation of tree-level and next-to-leading order differential cross sections, and their matching to parton shower simulations*, *JHEP* **07** (2014) 079, [[arXiv:1405.0301](#)].
- [72] J. Pumplin, D. R. Stump, J. Huston, H. L. Lai, P. M. Nadolsky, and W. K. Tung, *New generation of parton distributions with uncertainties from global QCD analysis*, *JHEP* **07** (2002) 012, [[hep-ph/0201195](#)].

- [73] G. Bélanger, F. Boudjema, A. Pukhov, and A. Semenov, *micrOMEGAs4.1: two dark matter candidates*, *Comput. Phys. Commun.* **192** (2015) 322–329, [[arXiv:1407.6129](#)].
- [74] **ATLAS** Collaboration, G. Aad et al., *Search for pair-produced third-generation squarks decaying via charm quarks or in compressed supersymmetric scenarios in pp collisions at $\sqrt{s} = 8$ TeV with the ATLAS detector*, *Phys. Rev.* **D90** (2014), no. 5 052008, [[arXiv:1407.0608](#)].
- [75] **CMS** Collaboration, V. Khachatryan et al., *Search for dark matter, extra dimensions, and unparticles in monojet events in proton-proton collisions at $\sqrt{s} = 8$ TeV*, *Eur. Phys. J.* **C75** (2015), no. 5 235, [[arXiv:1408.3583](#)].
- [76] E. Conte, B. Dumont, B. Fuks, and C. Wymant, *Designing and recasting LHC analyses with MadAnalysis 5*, *Eur. Phys. J.* **C74** (2014), no. 10 3103, [[arXiv:1405.3982](#)].
- [77] B. Dumont, B. Fuks, S. Kraml, S. Bein, G. Chalons, E. Conte, S. Kulkarni, D. Sengupta, and C. Wymant, *Toward a public analysis database for LHC new physics searches using MADANALYSIS 5*, *Eur. Phys. J.* **C75** (2015), no. 2 56, [[arXiv:1407.3278](#)].
- [78] D. Sengupta and G. Chalons, *Madanalysis 5 implementation of the ATLAS monojet analysis documented in arXiv:1407.0608*, *Phys. Rev. D.* **90**, 052008, .
- [79] D. Sengupta and G. Chalons, *Validation document for the Madanalysis 5 implementation of the ATLAS monojet analysis documented in arXiv:1407.0608*, *Phys. Rev. D.* **90**, .
- [80] T. Sjostrand, S. Mrenna, and P. Z. Skands, *PYTHIA 6.4 Physics and Manual*, *JHEP* **05** (2006) 026, [[hep-ph/0603175](#)].
- [81] S. Hoeche, F. Krauss, N. Lavesson, L. Lonnblad, M. Mangano, et al., *Matching parton showers and matrix elements*, [hep-ph/0602031](#).
- [82] **DELPHES 3** Collaboration, J. de Favereau, C. Delaere, P. Demin, A. Giammanco, V. Lematre, A. Mertens, and M. Selvaggi, *DELPHES 3, A modular framework for fast simulation of a generic collider experiment*, *JHEP* **02** (2014) 057, [[arXiv:1307.6346](#)].
- [83] M. Cacciari, G. P. Salam, and G. Soyez, *FastJet User Manual*, *Eur.Phys.J.* **C72** (2012) 1896, [[arXiv:1111.6097](#)].
- [84] M. Cacciari, G. P. Salam, and G. Soyez, *The Anti-k(t) jet clustering algorithm*, *JHEP* **0804** (2008) 063, [[arXiv:0802.1189](#)].
- [85] *ATLAS tunes of PYTHIA 6 and Pythia 8 for MC11*, Tech. Rep. ATL-PHYS-PUB-2011-009, CERN, Geneva, Jul, 2011.
- [86] A. L. Read, *Modified frequentist analysis of search results (The CL(s) method)*, in *Workshop on confidence limits, CERN, Geneva, Switzerland, 17-18 Jan 2000: Proceedings*, 2000.

- [87] A. L. Read, *Presentation of search results: The $CL(s)$ technique*, *J. Phys.* **G28** (2002) 2693–2704. [[11\(2002\)](#)].
- [88] M. R. Buckley, D. Feld, and D. Goncalves, *Scalar Simplified Models for Dark Matter*, *Phys. Rev.* **D91** (2015) 015017, [[arXiv:1410.6497](#)].
- [89] P. Harris, V. V. Khoze, M. Spannowsky, and C. Williams, *Constraining Dark Sectors at Colliders: Beyond the Effective Theory Approach*, *Phys. Rev.* **D91** (2015) 055009, [[arXiv:1411.0535](#)].
- [90] M. Chala, F. Kahlhoefer, M. McCullough, G. Nardini, and K. Schmidt-Hoberg, *Constraining Dark Sectors with Monojets and Dijets*, *JHEP* **07** (2015) 089, [[arXiv:1503.05916](#)].
- [91] *Search for New Phenomena in Dijet Mass and Angular Distributions with the ATLAS Detector at $\sqrt{s} = 13$ TeV*, Tech. Rep. ATLAS-CONF-2015-042, CERN, Geneva, Aug, 2015.
- [92] **CMS** Collaboration, V. Khachatryan et al., *Search for narrow resonances decaying to dijets in proton-proton collisions at $\sqrt{s} = 13$ TeV*, [arXiv:1512.01224](#).
- [93] O. Buchmueller, S. A. Malik, C. McCabe, and B. Penning, *Constraining Dark Matter Interactions with Pseudoscalar and Scalar Mediators Using Collider Searches for Multijets plus Missing Transverse Energy*, *Phys. Rev. Lett.* **115** (2015), no. 18 181802, [[arXiv:1505.07826](#)].
- [94] M. Spira, A. Djouadi, D. Graudenz, and P. M. Zerwas, *Higgs boson production at the LHC*, *Nucl. Phys.* **B453** (1995) 17–82, [[hep-ph/9504378](#)].
- [95] A. Djouadi, *The Anatomy of electro-weak symmetry breaking. I: The Higgs boson in the standard model*, *Phys. Rept.* **457** (2008) 1–216, [[hep-ph/0503172](#)].
- [96] **CMS** Collaboration, C. Collaboration, *Search for top quark partners with charge $5/3$ at $\sqrt{s} = 13$ TeV*, .
- [97] J. Hisano, K. Ishiwata, and N. Nagata, *Gluon contribution to the dark matter direct detection*, *Phys. Rev.* **D82** (2010) 115007, [[arXiv:1007.2601](#)].